RESEARCH PAPERS

Acta Cryst. (1996). B52, 217–222

Crystal and Magnetic Structure of Piezoelectric, Ferrimagnetic and Magnetoelectric Aluminium Iron Oxide $FeAlO_3$ from Neutron Powder Diffraction

F. BOUREE,[a] J. L. BAUDOUR,[b] E. ELBADRAOUI,[b] J. MUSSO,[c] C. LAURENT[d] AND A. ROUSSET[d]

[a]*Laboratoire Léon Brillouin, CE Saclay, 91191 Gif sur Yvette, France,* [b]*Laboratoire de Recherche sur les Matériaux à Finalités Spécifiques (EA 1356), Université de Toulon et du Var BP 132, 83957 La Garde CEDEX, France,* [c]*Laboratoire des Matériaux Multiphasés et Interfaces (EA 1357), Université de Toulon et du Var BP 132, 83957 La Garde CEDEX, France, and* [d]*Laboratoire de Chimie des Matériaux Inorganiques, URA CNRS 1311, Université Paul Sabatier, 31062 Toulouse, France*

(Received 16 January 1994; accepted 24 July 1995)

Abstract

The crystal structure of $FeAlO_3$ has been determined at T = 298 K by neutron diffraction, using polycrystalline samples prepared in a high state of purity. The space group is $Pna2_1$, Z = 8; a = 4.9839 (1), b = 8.5544 (2), c = 9.2413 (2) Å. The structure, which is isomorphous to that of $FeGaO_3$, can be described as a double combination of hexagonal and cubic closed packing of oxygen ions. There are four different cation sites labelled Fe1, Fe2 (predominantly occupied by iron), Al1 and Al2 (predominantly occupied by aluminium). The oxygen environment of Al1 forms an almost regular tetrahedron. The other sites have a distorted octahedral environment, especially irregular for Fe1 and Fe2. The fractions f_i of iron ions over the four cation sites are: f_1 = 0.78 (1), f_2 = 0.76 (1), f_3 = 0.10 (1) and f_4 = 0.34 (1). Neutron diffraction at T = 30 K reveals a classical Néel ferrimagnetism, the direction of easy magnetization being **a**, with strong '180° cation–anion–cation' superexchange antiferromagnetic interactions Fe1–O–Fe2 and Fe1–O–Al2 (Al2 being a site occupied by 0.34 Fe). The Néel sublattices are A = Fe1 + Al1 and B = Fe2 + Al2. The average magnetic moment per atom is weak (3.4 ± 0.3 μ_B) and the spontaneous magnetization at T = 30 K is extremely weak: 0.38 ± 0.17 μ_B per atom. Piezoelectricity probably originates in the bond arrangement of the four tetrahedral Al1 sites in the unit cell, each tetrahedron being oriented with an Al1—O bond parallel to the polar c axis.

1. Introduction

The orthorhombic phase of $FeAlO_3$ is piezoelectric, magnetoelectric and ferrimagnetic at low temperature (Macdonald, Gard & Glasser, 1967; Shieber, Frankel, Blum & Foner, 1967; Trooster & Dymanus, 1967; Mackenzie & Brown, 1984). High-field magnetization measurements on $FeAlO_3$ polycrystalline samples (Devaux, Rousset, Broto, Rakoto & Askenazy, 1990) show an extremely high magnetic anisotropy since at temperatures down to 4.2 K and in pulsed magnetic fields up to 37 T, the magnetic saturation of these samples is not reached. We have used neutron diffraction data obtained from $FeAlO_3$ powdered samples prepared in a high state of purity by new production methods (Devaux *et al.*, 1990) for determining the crystal (at T = 298 K) and magnetic (at T = 30 K) structures. We discuss the electric and magnetic properties of this crystal in terms of the packing of oxygen ions, cation distribution and magnetic interactions. A comparison is made with the isomorphous gallium iron oxide $FeGaO_3$.

2. Experimental and crystal data

The mixed oxalate precursor $(NH_4)_3[Fe_{0.5}Al_{0.5}(C_2O_4)_3]$ was prepared by coprecipitation from alcoholic medium. It was decomposed at 673 K and the resulting oxide solid solution was rapidly heated to 1653 K. After 2 h at this temperature, the specimen was quenched, giving rise to pure $FeAlO_3$, no other phase being detected by X-ray and electron diffraction. Neutron powder diffraction data* were collected at room temperature and at T = 30 K using the high-resolution diffractometer 3T2 at the Orphée reactor at the Laboratoire Léon Brillouin (Saclay, France). Full experimental conditions are reported in Table 1.

3. Refinement of the room-temperature structure

The structural scattering lengths used in the refinement were b_{Fe} = 9.45, b_{Al} = 3.449, b_O = 5.803 fm. The space group is $Pna2_1$; Z = 8. The initial atomic coordinates of the four independent heavy atoms and of the six independent O atoms were those proposed

* The numbered intensity of each measured point on the profile has been deposited with the IUCr (Reference: BR0041). Copies may be obtained through The Managing Editor, International Union of Crystallography, 5 Abbey Square, Chester CH1 2HU, England.

Table 1. *Experimental details*

	298 K	30 K
Crystal data		
Chemical formula	$AlFeO_3$	$AlFeO_3$
Chemical formula weight	130.83	130.83
Cell setting	Orthorhombic	Orthorhombic
Space group	$Pna2_1$	$Pna2_1$
a (Å)	4.9839 (1)	4.9792 (1)
b (Å)	8.5544 (2)	8.5466 (2)
c (Å)	9.2413 (2)	9.2345 (2)
V (Å^3)	394	393
Z	8	8
D_x (Mg m^{-3})	4.411	4.423
Radiation type	Neutron	Neutron
Wavelength (Å)	1.2268	1.2268
θ range (°)	6–109	6–109
μ (mm^{-1})	0.003	0.003
Temperature (K)	298	30
Data Collection		
Diffractometer	3T2 LLB Saclay	3T2 LLB Saclay
Sample container	Vanadium holder	Vanadium holder
Monochromator	Ge 335	Ge 335
Instrument geometry	20 ^{3}He detectors	20 ^{3}He detectors
θ_{max} (°)	109	109
2θ step (°)	0.05	0.05
Refinement		
Background	Polynomial function	Polynomial function
R	0.0317	0.0352
wR	0.0416	0.0473
R_{exp}	0.0233	0.0252
$R_I = \Sigma(I_i - I_{ci})/\Sigma I_i$	0.0358	0.0274
Magnetic R factor	–	0.0778
χ^2	3.04	3.53
No. of parameters used	50	54
Weighting scheme	$w_i = 1/\sigma_i^2$, $\sigma_i^2 = y_i$	$w_i = 1/\sigma_i^2$, $\sigma_i^2 = y_i$
Full width at half-maximum	$u\tan^2\theta + v\tan\theta + w$	$u\tan^2\theta + v\tan\theta + w$
Analytic function for profile	Gaussian shape	Gaussian shape
$(\Delta/\sigma)_{max}$	0.070	0.070
Computer programs		
Cell refinement	*Fullprof* (Rodriguez-Carvajal, 1990)	*Fullprof* (Rodriguez-Carvajal, 1990)

Table 2. *Final positional and displacement parameters, and occupancy factors of $FeAlO_3$ at room temperature and at $T = 30$ K, and magnetic moments at $T = 30$ K*

f = fraction of iron at the lattice sites; M = magnetic moment per iron ion.

Site	T (K)	x	y	z	B_{iso} (Å^2)	Occupancy by Fe	Occupancy by Al	Mf (μ_B)	M (μ_B)
Fe1	300	0.1850 (7)	0.1518 (4)	0.5827 (5)	0.20 (6)	0.777 (13)	0.223 (13)		
Fe1	30	0.1850 (7)	0.1525 (4)	0.5822 (5)	0.09 (9)	0.803 (30)	0.197 (30)	−2.59 (22)	−3.23 (30)
Fe2	300	0.6731 (7)	0.0334 (3)	0.7982 (5)	0.38 (6)	0.764 (12)	0.236 (12)		
Fe2	30	0.6725 (7)	0.0330 (3)	0.7981 (6)	0.14 (8)	0.751 (22)	0.249 (22)	+2.68 (19)	+3.57 (27)
Al1	300	0.1729 (12)	0.1528 (8)	0.0000 (0)	0.56 (10)	0.095 (9)	0.905 (9)		
Al1	30	0.1727 (12)	0.1528 (8)	0.0000 (0)	0.36 (11)	0.105 (11)	0.895 (11)	−0.36 (10)	−3.43 (103)
Al2	300	0.8155 (10)	0.1600 (6)	0.3035 (7)	0.60 (9)	0.340 (12)	0.660 (12)		
Al2	30	0.8132 (11)	0.1602 (6)	0.3037 (7)	0.25 (10)	0.310 (15)	0.690 (15)	+1.00 (13)	+3.23 (45)
O1	300	0.9822 (9)	0.3230 (5)	0.4211 (7)	0.58 (2)				
O1	30	0.9838 (10)	0.3228 (5)	0.4213 (7)	0.40 (2)				
O2	300	0.5101 (9)	0.4911 (6)	0.4294 (8)	0.58 (2)				
O2	30	0.5085 (9)	0.4902 (6)	0.4303 (8)	0.40 (2)				
O3	300	0.6581 (12)	1.0019 (5)	0.2005 (7)	0.58 (2)				
O3	30	0.6589 (12)	1.0021 (5)	0.2002 (7)	0.40 (2)				
O4	300	0.1555 (13)	0.1629 (5)	0.1948 (6)	0.58 (2)				
O4	30	0.1548 (14)	0.1636 (5)	0.1944 (7)	0.40 (2)				
O5	300	0.8451 (12)	0.1683 (6)	0.6727 (7)	0.58 (2)				
O5	30	0.8436 (13)	0.1686 (6)	0.6722 (8)	0.40 (2)				
O6	300	0.5089 (12)	0.1727 (6)	0.9409 (7)	0.58 (2)				
O6	30	0.5091 (13)	0.1728 (6)	0.9404 (7)	0.40 (2)				

for the isostructural $FeGaO_3$ in the precedent studies (Abrahams, Reddy & Bernstein, 1965; Bertaut, Bassi, Buisson, Chappert, Delapalme, Pauthenet, Rebouillat & Aleonard, 1966). Then all positional parameters (except z of Al1 = 0), isotropic temperature factors (imposing the same value for all O atoms) and the occupancy factors for the heavy atoms were varied. The other variable parameters were an overall scale factor, usual u, v and w parameters (defined in Table 1), an asymmetry parameter determining the shape of the Bragg peaks and the zero point for the Bragg angles. The R factors converged quickly to $Rp = 0.0317$ and $Rwp = 0.0416$. The strongest correlations (0.96) occurred between the occupancy and temperature factor of Fe1 and the z coordinate and temperature factor of the same atom.

Anisotropic thermal motion refinement was then allowed for the heavy atoms, retaining isotropic temperature factors for the O atoms. No significant improvement was noted. Nor was any improvement found by allowing anisotropic thermal motion for only Al2, the atom exhibiting the largest thermal motion. The final atomic coordinates after isotropic refinement are shown in Table 2. In Fig. 1(*a*) a comparison of the experimental and calculated neutron diffraction data is presented. A representation of the structure projected along **a** is given in Fig. 2.

4. Oxygen packing, occupancy factors, polyhedral sharing and characteristic temperature

As in $FeGaO_3$, the structure of $FeAlO_3$ can be described as a double hexagonal (hc) close-packed array of oxygen ions (Fig. 3), *i.e.* a combination of hexagonal and cubic close packing: the repeat of the layers along **z** is in the form *ABCB...ABCB*, where *ABC* designates cubic close packing, each oxygen layer consisting of a pseudo-hexagonal array. The heavy atoms also lie in four layers along **z**, alternating with oxygen layers, the Fe1–Al1 layers being very puckered (Fig. 2).

There are four different cation sites labelled Fe1, Fe2, Al1 and Al2, the occupation factors permitting the iron sites to be occupied to a smaller extent by aluminium and the aluminium sites by iron. The oxygen environment of Al1 forms an almost regular tetrahedron. The three other sites have a distorted octahedral environment, especially

the oxygen environment of Fe1 and Fe2 is very irregular (Table 3). The distribution of iron ions over the cation sites has been determined accurately. If f_1, f_2, f_3 and f_4 are the fractions of iron ions at the lattice sites Fe1, Fe2, Al1 and Al2, respectively, the total occupancy of each site being constrained to be 1.0, the values of f_i are: f_1 = 0.78 (0.01), f_2 = 0.76 (0.01), f_3 = 0.10 (0.01) and f_4 = 0.34 (0.01).

This distribution corresponds to the formula $Fe_{0.99}Al_{1.01}O_3$, showing no significant departure from the nominal composition $FeAlO_3$. These results confirm the structural features deduced from the Mössbauer spectrum by Mackenzie & Brown (1984), who conclude that iron occupies both octahedral and tetrahedral sites and that ~10% of the tetrahedral sites (Al1 sites) are occupied by Fe^{3+}, the remainder being occupied by Al^{3+}.

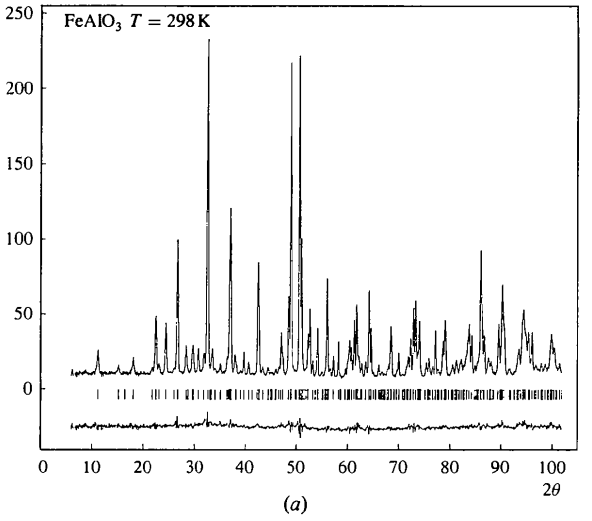

Fig. 1. Diffractometer patterns of $FeAlO_3$, showing comparison between experimental and calculated data: (*a*) T = 298 and (*b*) T = 30 K.

The large difference between octahedral radii of Fe^{3+} and Al^{3+} ions, 0.645 and 0.535 Å, respectively (Shannon, 1976), together with disorder in the occupation of cation sites, especially for octahedral sites, leads to a local deformation of the lattice.

There are six crystallographically different oxygen ions in the $FeAlO_3$ structure, denoted O1–O6 (Fig. 2). They can be divided into two groups:

Type I: O3, O5 and O6 each have only three cations as nearest neighbours.

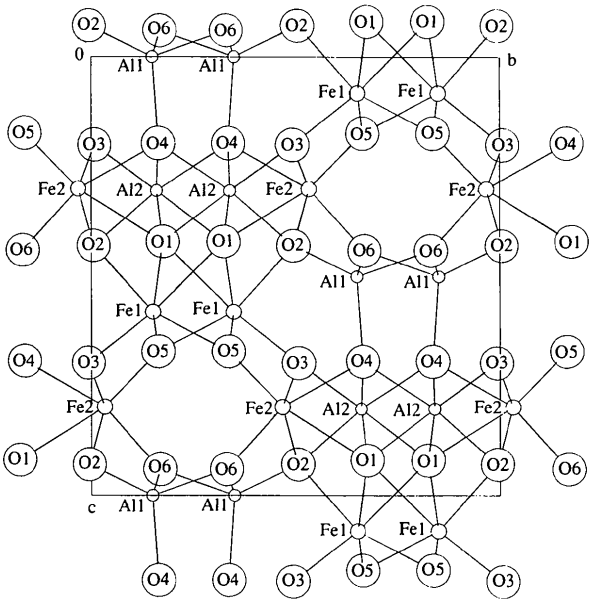

Fig. 2. Structure of $FeAlO_3$ projected along **a**.

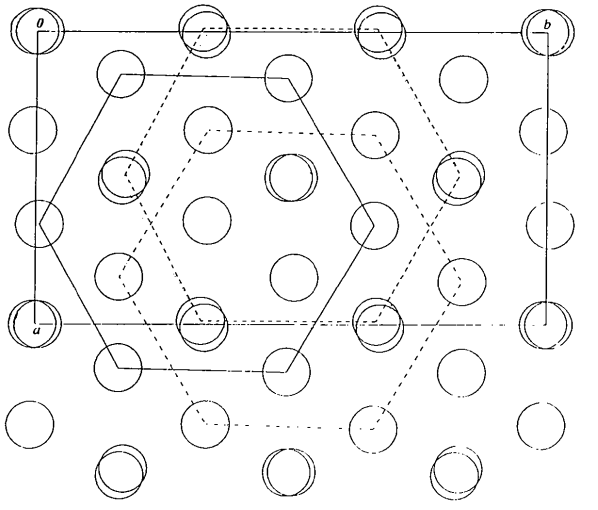

Fig. 3. O-atom array, projected along **c**. Hexagons have been drawn for each layer, corresponding to *ABCB* packing; *A*: solid line (z = 0.18), *B*: broken line (z = 0.43), *C*: mixed line (z = 0.68), *B*: dotted line (z = 0.93).

Type II: O1, O2 and O4 have four or five (O1) nearest-neighbour cations.

The bond lengths of type II oxygens (O_{II}) with the cations at the Fe1 and Fe2 sites are larger ($2.02 < d < 2.32$ Å) than the bond lengths of type I oxygens O_I ($1.85 < d < 1.96$ Å). At the Fe1 and Fe2 sites the O_I—Fe—O_I angles are larger ($93.1 < \alpha < 103.7°$) than the O_{II}—Fe—O_{II} angles ($74.5 < \alpha < 82.6$; Table 3).

Sharing of edges between octahedra is shown in Table 4 and will be discussed with the magnetic structure. The Al1 tetrahedron shares O atoms only at the corners, no edge sharing occurs between tetrahedra and octahedra.

The characteristic temperature θ of aluminium iron oxide may be computed using the expression $B = (6h^2/mkTx^2)(\Phi(x) + x/4)$, where h is Planck's constant, k Boltzmann's constant, $x = \theta/T$, $m = 4.34 \times 10^{-23}$ g atom^{-1} is the average mass of an atom in the unit cell, $B = 0.521$ Å^2 is the average thermal parameter at $T = 300$ K and $\Phi(x) = (1/x)[\int_0^x y\,dy/(e^y - 1)]$. $\theta = 521$ K in $FeAlO_3$, which can be compared with $\theta = 534$ K in $FeGaO_3$ (Abrahams *et al.*, 1965). However, it must be noted that the B factor of each atomic site contains contributions from both thermal motion and static structural disorder, the latter being introduced by the large difference in ionic radii of Fe^{3+} and Al^{3+}. Consequently, θ is probably underestimated.

5. Structure and piezoelectricity

It has been proposed in the case of $Fe_{1.15}Ga_{0.85}O_3$ (Abrahams *et al.*, 1965) that the piezoelectric effect originates in the bond arrangement of the metal atoms located on the tetrahedral sites in the cell; this bond arrangement being analogous to that in the classical example of zinc sulfide. The same bond disposition is found in $FeAlO_3$, one of the tetrahedral bonds (Al1—O4) being parallel, or almost so (at $\pm 4°$), to the polar c axis, which is the largest axis (Fig. 2). Pressure along the c axis causes a compression in the Al1—O4 bonds and for the remaining three Al1—O bonds alters their angle with the polar axis, inducing a polarization.

6. The magnetic structure (T = 30 K)

$FeAlO_3$ undergoes a ferrimagnetic phase transition at $T_c \simeq 280$ K. We have determined the $FeAlO_3$ magnetic structure at low temperature from neutron powder diffraction at $T = 30$ K. The magnetic unit cell is identical to the chemical one (orthorhombic space group $Pna2_1$). Compared with room-temperature refinements, four new parameters are added, giving the magnetic moments f_iM_i on each metal site (f_i iron occupancy factor, M_i moment per iron atom). The best fit between observed and calculated magnetic intensities (Rietveld profile refinement of the $T = 30$ K neutron powder

Table 3. *Distances (Å) and angles (°) in the octahedra centred on Fe1, Fe2 or Al2 and in the tetrahedra centred on Al1*

The Fe—O(i) or Al—O(i) distances are on the diagonal, above it are the O(i)—O(j) distances and under it are O(i)—Fe—O(j) or O(i)—Al—O(j) angles

Fe1

Average Fe1—O(i) distance: 2.032 (3) Å; average deviation: 0.135 (3) Å

Average ~ 180° O(i)—Fe1—O(j) angle: 164.7 (2)°; average deviation: 15.3 (2)°

Average ~ 90° O(i)—Fe1—O(j) angle: 89.4 (1)°; average deviation: 8.0 (1)°

Fe1	O3^{i}	O5^{ii}	O5^{iii}	O2^{iii}	O1^{iii}	O1^{ii}
O3	1.878 (7)	2.884 (8)	2.866 (7)	3.003 (9)	3.082 (8)	4.197 (8)
O5	99.8 (3)	1.892 (7)	2.857 (8)	2.755 (9)	3.936 (8)	2.761 (8)
O5	97.9 (3)	97.0 (3)	1.922 (7)	3.933 (8)	2.761 (8)	2.947 (9)
O2	99.1 (3)	88.1 (3)	161.1 (4)	2.064 (8)	2.759 (6)	2.692 (7)
O1	100.9 (3)	158.4 (3)	86.2 (3)	82.6 (3)	2.114 (7)	2.788 (7)
O1	174.6 (3)	81.1 (3)	87.4 (3)	75.4 (2)	77.7 (2)	2.323 (7)

Fe2

Average Fe2—O(i) distance: 2.018 (3) Å; average deviation: 0.115 (3) Å

Average ~ 180° O(i)—Fe2—O(j) angle: 162.6 (2)°; average deviation: 17.4 (2)°

Average ~ 90° O(i)—Fe2—O(j) angle: 89.4 (1)°; average deviation: 7.2 (1)°

Fe2	O5	O3^{i}	O6	O2^{iv}	O4^{v}	O1^{iv}
O5	1.847 (7)	2.912 (8)	2.992 (9)	2.906 (9)	2.841 (7)	4.081 (8)
O3	101.8 (3)	1.905 (7)	2.803 (9)	3.861 (8)	2.859 (8)	2.677 (8)
O6	103.7 (3)	93.1 (3)	1.956 (7)	2.858 (7)	4.026 (8)	2.997 (7)
O2	97.2 (3)	158.7 (3)	91.8 (3)	2.023 (7)	2.638 (9)	2.759 (6)
O4	91.4 (3)	90.6 (3)	163.3 (3)	79.2 (3)	2.112 (6)	2.653 (8)
O1	165.9 (3)	79.4 (2)	90.2 (3)	79.9 (2)	74.5 (2)	2.264 (6)

Al1

Average Al1—O(i) distance: 1.785 (4) Å; average deviation: 0.010 (4) Å

Average ~ 109.47° O(i)—Al1—O(j) angle: 109.3 (2)°; average deviation: 3.7 (2)°

Al1	O6^{vi}	O2^{vii}	O6^{viii}	O4
O6	1.770 (8)	3.019 (7)	2.821 (8)	2.935 (9)
O2	116.6 (4)	1.780 (8)	2.879 (7)	2.976 (9)
O6	105.0 (4)	107.6 (4)	1.787 (8)	2.832 (8)
O4	110.4 (4)	112.2 (4)	104.1 (4)	1.805 (6)

Al2

Average Al2—O(i) distance: 1.953 (3) Å; average deviation: 0.041 (3) Å

Average ~ 180° O(i)—Al2—O(j) angle: 174.2 (2)°; average deviation: 5.8 (2)°

Average ~ 90° O(i)—Al2—O(j) angle: 89.9 (1)°; average deviation: 4.7 (1)°

Al2	O3^{ix}	O1	O4^{x}	O4^{xi}	O1^{iii}	O2^{xi}
O3	1.830 (8)	3.783 (7)	2.836 (8)	2.868 (6)	2.677 (8)	2.749 (9)
O1	177.5 (4)	1.954 (7)	2.645 (8)	2.663 (8)	2.788 (7)	2.692 (7)
O4	96.5 (4)	84.8 (3)	1.970 (8)	2.904 (9)	3.955 (8)	2.638 (9)
O4	97.4 (4)	84.7 (3)	94.5 (3)	1.985 (7)	2.645 (8)	3.963 (8)
O1	88.9 (3)	90.0 (3)	174.5 (4)	83.4 (3)	1.990 (8)	2.999 (6)
O2	91.9 (3)	86.1 (3)	83.5 (3)	170.6 (4)	97.7 (3)	1.992 (8)

Symmetry codes: (i) $1-x, 1-y, z+\frac{1}{2}$; (ii) $x-1, y, z$; (iii) $x-\frac{1}{2}, \frac{1}{2}-y, z$; (iv) $\frac{3}{2}-x, y-\frac{1}{2}, z+\frac{1}{2}$; (v) $1-x, -y, z+\frac{1}{2}$; (vi) $x, y, z-1$; (vii) $\frac{1}{2}-x, y-\frac{1}{2}, z-\frac{1}{2}$; (viii) $x-\frac{1}{2}, \frac{1}{2}-y, z-1$; (ix) $x, y-1, z$; (x) $x+1, y, z$; (xi) $x+\frac{1}{2}, \frac{1}{2}-y, z$.

Table 4. *Edges sharing between octahedra*

The table gives the distances (Å) between cations in octahedra sharing a common edge. There is no particular rule for the relative orientation of the moments of these cations, the ~ 90° cation–anion–cation magnetic interactions being weak.

	Edges shared		Fe1		Fe2		Al2
Octahedra	Total number		5		4		7
Fe1	5	2 edges shared	3.005 (5)	1 edge shared	3.150 (6)	2 edges shared	3.110 (8)
		with Fe1	3.005 (5)	with Fe2		with Al2	3.171 (7)
Fe2	4	1 edge shared	3.150 (6)			3 edges shared	2.944 (6)
		with Fe1				with Al2	3.196 (6)
							3.039 (6)
Al2	7	2 edges shared	3.110 (8)	3 edges shared	2.944 (6)	2 edges shared	2.930 (7)
		with Fe1	3.171 (7)	with Fe2	3.196 (6)	with Al2	2.930 (7)
					3.039 (6)		

diffraction data; Fig. 1*b*) is obtained for a collinear ferrimagnetic structure, with Fe^{3+} magnetic moments respectively parallel and antiparallel to **a**, the shortest axis of the crystal structure. All Fe^{3+} ions on a 4(*a*) site have the same magnetic moment, within standard deviations (M_1 for Fe1, M_2 for Fe2, M_3 for Fe^{3+} in the Al1 site and M_4 for Fe^{3+} in the Al2 site), the algebraic values of f_iM_i (sequence + − + −) being given in Table 2. This magnetic structure, analogous to the magnetic structure of $Fe_{1.15}Ga_{0.85}O_3$ (Bertaut *et al.*, 1966), is mainly determined by the strong '180° cation–anion–cation' superexchange antiferromagnetic interactions (Goodenough, 1966) Fe1–O1–Fe2 and Fe1–O1–Al2, Al2 designating a site occupied by 0.31 Fe (see Table 5; Fig. 4). This table gives Fe^{3+}—O^{2-}—Fe^{3+} angles larger than 115° for cations sharing a common corner of their oxygen coordination polyhedra: the Fe^{3+} on each side have opposite magnetic moments, except the lowest value of the angle. Fe^{3+} cations sharing a common edge of their oxygen coordination polyhedra (see Table 4) are not so strongly magnetically correlated, '≃ 90° Fe^{3+}–O^{2-}–Fe^{3+}' superexchange magnetic interactions being weak (Goodenough, 1966).

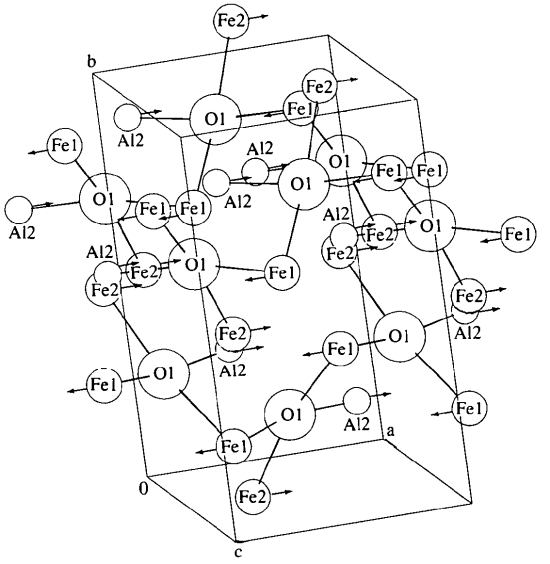

Fig. 4. The '~180° cation–anion–cation' antiferromagnetic interactions Fe1—O—Fe2 (166°) and Fe1— O—Al2 (164°). Al2 is a site occupied by 0.3 Fe.

Table 5. *Corner sharing between polyhedra*

The table gives the metal–anion–metal angles larger than 115° in decreasing order. α is the angle A—O—B. Due to the strong '180° cation–anion–cation' superexchange antiferromagnetic interactions, the Fe^{3+} cations A and B have their spins oppositely oriented, except for the smallest angle of the list.

A—O—B	α (°)
Fe1—O1—Fe2	166.4 (3)
Fe1—O1—Al2	164.3 (3)
Fe1—O5—Fe2	130.2 (3)
Fe1—O3—Al2	129.8 (4)
Fe1—O5—Fe2	125.4 (4)
Al1—O4—Al2	123.3 (4)
Al1—O6—Fe2	123.0 (4)
Al1—O6—Fe2	121.6 (4)
Fe1—O3—Fe2	121.6 (3)
Al1—O4—Al2	121.4 (4)
Al1—O2—Fe2	118.7 (3)
Al1—O2—Al2	117.9 (3)
Fe1—O2—Al1	115.2 (4)

The T = 30 K refined parameters are given in Table 2. The occupation numbers f_i are identical at 30 and 300 K (within standard deviations). The mean Fe^{3+} magnetic moment at T = 30 K is 3.4 ± 0.3 μ_B, a value lower than expected (g_JJ = 5 μ_B): this is probably due to the chemical disorder on the cations sites, magnetic linkages between Fe^{3+} ions being randomly disrupted by non-magnetic Al^{3+} ions. The spontaneous magnetization deduced from the T = 30 K neutron powder diffraction data (Table 2) is parallel to **a** and equal to 0.38 ± 0.17 μ_B/Fe^{3+}, in agreement with the 0.4 μ_B magnetization measurement of Devaux *et al.* (1990).

References

Abrahams, S. C., Reddy, J. M. & Bernstein , J. L. (1965). *J. Chem. Phys.* **42**, 3957–3970.

Bertaut, E. F., Bassi, G., Buisson, G., Chappert, J., Delapalme, A., Pauthenet, R., Rebouillat, H. P. & Aleonard, R. (1966). *J. Phys.* **27**, 433–448.

Devaux, X., Rousset, A., Broto, J. M., Rakoto, H. & Askenazy, S. (1990). *J. Mat. Sci. Lett.* **9**, 371–372.

Goodenough, J. B. (1966). *Magnetism and the Chemical Bond*, edited by F. A. Cotton, pp. 168–180. New York: John Wiley & Sons.

Macdonald, J., Gard, J. A. & Glasser, F. P. (1967). *J. Inorg. Nucl. Chem.* **29**, 661–671.

Mackenzie, K. J. D. & Brown, I. W. M. (1984). *J. Mat. Sci. Lett.* **3**, 159–161.

Rodriguez-Carvajal, J. (1990). *Fullprof. A Program for Rietveld Refinement and Pattern Matching Analysis.* Abstracts of the Satellite Meeting on Powder Diffraction of the XV Congress of the IUCr, p. 127.

Shannon, R. D. (1976). *Acta Cryst.* A**32**, 751–767.

Shieber, M., Frankel, R. B., Blum, N. A. & Foner, S. (1967). *J. Appl. Phys.* **38**, 1282–1283.

Trooster, J. M. & Dymanus, A. (1967). *Phys. Status Solidi*, **24**, 487–499.